



Published in final edited form as:

Oncogene. 2015 April 23; 34(17): 2167–2177. doi:10.1038/onc.2014.161.

Ligand associated ERBB2/3 activation confers acquired resistance to FGFR inhibition in FGFR3 dependent cancer cells

Jun Wang, Oliver Mikse, Rachel G. Liao, Yvonne Li, Li Tan, Pasi A. Janne, Nathanael S. Gray, Kwok-kin Wong, and Peter S. Hammerman

¹Department of Medical Oncology, Dana-Farber Cancer Institute, Boston, MA

²Department of Integrative Medicine and Neurobiology, Shanghai Medical College, Fudan University, Shanghai, China

³Broad Institute of Harvard and MIT, Cambridge MA

⁴Department of Biological Chemistry and Molecular Pharmacology, Harvard Medical School, Boston MA

⁵Belfer Institute of Applied Cancer Sciences, Boston, MA

Abstract

Somatic alterations of Fibroblast Growth Factor Receptors (FGFRs) have been described in a wide range of malignancies. A number of anti-FGFR therapies are currently under investigation in clinical trials for subjects with *FGFR* gene amplifications, mutations and translocations. Here, we develop cell line models of acquired resistance to FGFR inhibition by exposure of cell lines harboring *FGFR3* gene amplification and translocation to the selective FGFR inhibitor BGJ398 and multi-targeted FGFR inhibitor ponatinib. We show that the acquisition of resistance is rapid, reversible and characterized by an epithelial to mesenchymal transition (EMT) and a switch from dependency on *FGFR3* to *ERBB* family members. Acquired resistance was associated with demonstrable changes in gene expression including increased production of ERBB2/3 ligands which were sufficient to drive resistance in the setting of *FGFR3* dependency but not dependency on other *FGFR* family members. These data support the concept that activation of *ERBB* family members is sufficient to bypass dependency on *FGFR3* and suggest that concurrent inhibition of these two pathways may be desirable when targeting *FGFR3* dependent cancers.

Keywords

FGFR3 translocation; FGFR inhibitors; cancer genomics; acquired resistance

Users may view, print, copy, and download text and data-mine the content in such documents, for the purposes of academic research, subject always to the full Conditions of use:http://www.nature.com/authors/editorial_policies/license.html#terms

*Correspondence to: Dana-Farber Cancer Institute 450 Brookline Ave Dana 810A Boston, MA 02215 617-632-3000 (p) 617-582-7880 (f) phammerman@partners.org.

Disclosure of Potential Conflicts of Interest Potential Conflicts of Interest: P.S.H. reports consulting fees from ARIAD, ImClone, Janssen and Molecular MD.

Supplementary Information accompanies the paper on the *Oncogene* website.

Potential Conflicts of Interest: P.S.H. reports consulting fees from ARIAD, ImClone, Janssen and Molecular MD.

Introduction

The Fibroblast Growth Factors (FGFs) and their cognate receptors (FGFRs) comprise a signaling pathway which plays a critical role in many physiological processes, including cell proliferation, differentiation, migration and survival. FGF signaling is fundamental in embryonic development as well as in regulation of angiogenesis and wound healing in adults. The FGF family consists of 22 ligands, among them 18 ligands which exert their actions through four highly conserved transmembrane tyrosine kinase receptors: FGFR1, FGFR2, FGFR3 and FGFR4. Stimulation of the receptors by ligand binding promotes receptor dimerization and activation of several signaling cascades, including the MAPK and PI3K pathways^{1, 2, 3}.

Aberrant activity of FGFRs has been identified in diverse cancer types. FGFRs are activated by gene amplification, point mutation and chromosomal translocation. Amplification of *FGFR1* is observed in squamous cell lung cancer^{4, 5}, breast cancer⁶, and amplification of *FGFR2* is found in gastric⁷ and breast cancers⁸. Activating point mutations of *FGFRs* are observed in bladder cancers⁹, endometrial cancers¹⁰ and lung squamous cell carcinoma¹¹. Translocations coupled with amplifications and mutations of *FGFR3* have been observed in multiple myeloma^{12, 13}.

More recently, high-throughput sequencing technologies have identified a variety of *FGFR* gene fusions. *FGFR1-TACC1* and *FGFR3-TACC3* fusions have been identified in glioblastoma¹⁴ and *FGFR3-TACC3* fusions were found in bladder carcinomas and in lung and head and neck squamous cell carcinomas^{15, 16, 17}. Pre-clinical studies have shown that cells harboring FGFR fusions demonstrate dependency on FGFR-mediated signaling, suggesting that cancer patients with FGFR fusions may benefit from targeted FGFR kinase inhibition^{14, 18}. Clinical trials to test this hypothesis are underway (www.clinicaltrials.gov).

As preclinical studies have suggested that activated FGFRs are potential targets for cancer therapy¹⁹, and several selective FGFR inhibitors are under investigation in clinical trials^{1, 2} with early reports demonstrating clinical efficacy in *FGFR1* amplified breast cancer²⁰ and lung cancer²¹. NVP-BGJ398 (BGJ398) is an example of a selective, potent and orally bioavailable inhibitor of FGFR1/2/3 (ref. 22). BGJ398 inhibits the proliferation of various FGFR-dependent cell lines at nanomolar concentrations including lung and breast cancers harboring *FGFR1* amplification, gastric cancers harboring *FGFR2* amplification and bladder cancers with *FGFR3* mutations and/or amplifications²³.

While FGFR inhibition shows considerable clinical promise it is expected that patients who initially respond to FGFR inhibitors will become refractory due to the development of acquired resistance²⁴. Previous studies have shown that stimulation of some *FGFR2*- and *FGFR3*-dependent cell lines with the Hepatocyte Growth Factor (HGF) decreases sensitivity to FGFR inhibitors and that concurrent inhibition of the Epidermal Growth Factor Receptor (EGFR) with pharmacologic inhibitors or RNA interference can potentiate the activity of FGFR inhibitors in some cell lines^{25, 26}. Additionally, long-term exposure of a FGFR-dependent myeloma cell line to AZD4547 led to the acquisition of a second site (gatekeeper) mutation in *FGFR3* (ref. 27). Despite these initial observations, the mechanisms governing

the acquisition of resistance to FGFR inhibitors remain poorly understood. Therefore, an improved understanding of the molecular mechanisms of acquired resistance to FGFR inhibitors will likely provide valuable insight into how best to use this class of agents.

To study potential mechanisms of acquired resistance to selective FGFR inhibition, we established resistant cells *in vitro* following long-term exposure to BGJ398. We selected the RT112 bladder cancer cell line which harbors both *FGFR3* amplification and a *FGFR3-TACC3* fusion as our initial model. Through screening of the activity of 42 membrane receptor tyrosine kinases (RTKs) and mRNA sequencing, we identified that ERBB2 and ERBB3 are activated in the resistant cells in a ligand dependent fashion. Acquired resistance to FGFR inhibition developed rapidly and was characterized by an Epithelial to Mesenchymal Transition (EMT) along with a switch in dependency from FGFR to ERBB receptor signaling. These results were specific to cell lines with dependency on *FGFR3* and were recapitulated using a second FGFR kinase inhibitor, ponatinib.

Results

Phenotypic changes associated with the acquisition of resistance to the pan-FGFR inhibitor BGJ398 in the RT112 cell line

RT112 cells, which harbor both *FGFR3* amplification and the *FGFR3-TACC3* fusion, were rendered resistant to BGJ398 by a series of step-wise increases in drug concentration starting at 4nM (the approximate IC₅₀) until the cells were able to proliferate in 1μM BGJ398. We selected this cell line for our studies given its dependence on the *FGFR3* fusion and anecdotal reports of clinical efficacy of FGFR kinase inhibitors in patients with *FGFR3* fusions. These cells were termed BGJ398 RS (BGJ398 Resistant Stepwise). 1μM was selected as the target final concentration as it is the approximate maximal serum concentration observed in animal and Phase I studies of BGJ398. The cell lines were both insensitive to BGJ398 (Fig.1A) and a second, less specific, FGFR kinase inhibitor ponatinib (Fig.S1).

We noted that the BGJ398 RS cells underwent a morphologic change during their acquisition of resistance to BGJ398 from a densely packed adherent layer of small cells to a spindle-like morphology with loss of intercellular adhesion, increased intercellular separation and increased formation of pseudopodia, suggestive of an EMT (Fig.1B). EMT has been previously observed in lung cancer in the context of acquired resistance to EGFR inhibitors²⁸, prompting us to test whether this transition may also have occurred in our system. We performed real-time PCR analysis of genes previously associated with EMT. We observed that mRNA levels of E-cadherin were downregulated in BGJ398 RS cells and N-cadherin and fibronectin expression were upregulated, consistent with an EMT phenotype (Fig.1C) and levels of *PLAU*, *PLAUR*, *SNAIL* and *SLUG* were slightly but not significantly increased (data not shown). Immunoblots similarly demonstrated a decrease in the protein levels of the epithelial marker E-cadherin and an increase in the mesenchymal markers N-cadherin and fibronectin (Fig.1D).

Enhanced cellular migration and invasion are other hallmarks of advanced cancer and metastasis²⁹. We therefore assessed migration and invasion using scratch and matrigel

invasion assays. BGJ398 RS cells displayed enhanced migration potential in a scratch assay in the presence or absence of BGJ398 treatment as compared to the parental RT112 cell line (Fig.1E, DMSO treated cells), though the cells still demonstrated some sensitivity to BGJ398 in this assay, suggesting that there is ongoing FGFR-dependent signaling in the resistant state (Fig.1E, BGJ398 treated cells). Similarly, BGJ398 RS demonstrated greater invasion in matrigel coated Boyden chambers as compared to the parental line both in the presence and absence of BGJ398—but as in Fig.1E, resistant cells retained some sensitivity to BGJ398 (Fig.1F).

Activation of ERBB2 and ERBB3 in BGJ398 RS cells

We sought to investigate the molecular underpinnings of acquired resistance to BGJ398 in RT112 cells. Given that other studies have implicated the *MET* gene as a critical mediator of resistance to FGFR inhibitors^{25, 30, 31}, we investigated whether levels of total or phospho-MET might be increased in BGJ398 RS. We observed that p-MET was undetectable in the BGJ398 resistant cells and total MET levels slightly decreased (Fig.S2); however, cells resistant to ponatinib demonstrated stability of p-MET and total MET protein (Fig.S2).

We next queried the activation status of many cancer-related RTKs using a phospho-receptor tyrosine kinase array to compare the phosphorylation status of 42 RTKs in RT112 parental cells, RT112 cells treated acutely with BGJ398, and BGJ398 RS cells. We identified two RTKs with increased phosphorylation when comparing the treated and parental lines, ERBB2 and ERBB3 (Fig.2A). ERBB2 was increased in RT112 cells treated with BGJ398 in the acute setting (1h) and both ERBB2 and ERBB3 were increased in the final resistant cell populations both in the presence and absence of BGJ398 treatment. Strong phospho-EGFR was maintained in both cell lines and IGF1R was decreased in the resistant line as compared to the parental.

To confirm these results, we performed immunoblots on RT112 cells treated with BGJ398 over a 24-hour timecourse. We observed that p-FRS2 and p-FGFR levels decreased with BGJ398 treatment as would be expected (Fig.2B). While levels of phospho- and total EGFR did not change to a substantial degree with BGJ398 treatment, both p-ERBB2 and p-ERBB3 were induced at 12 hours following treatment (Fig.2B). Similar immunoblots were performed in the BGJ398 RS and ponatinib RS lines; these results are presented in Fig.S3. Here we noted that p-FRS2 levels were below the limits of detection in the resistant lines and that basal levels of p-ERBB2 and p-ERBB3 were higher in the BGJ398 RS and ponatinib RS lines (Fig.S3). p-AKT was also maintained at an increased level of phosphorylation in the resistant lines in the setting of pharmacologic inhibition of FGFRs (Fig.S3).

As these data suggested that ERBB family members may be activated by treatment with FGFR inhibitors and may be playing a role in acquired resistance, we assessed the dimerization status of ERBB family members in RT112 cells treated with BGJ398. EGFR, ERBB2 and ERBB3 are known to form homo- or heterodimers when stimulated by their ligands^{32, 33}. We performed co-immunoprecipitation studies and observed an increase in heterodimerization of ERBB2 and ERBB3 in the parental cells after 1 μ M BGJ398 stimulation for 24 hours as compared to untreated RT112 cells (Fig.2C), again suggesting a

possible role for ERBB2 and ERBB3 signaling in drug-treated parental cells. The immunoprecipitation assays detected a ERBB2/ERBB3 complex when ERBB2 was immunoprecipitated followed by a ERBB3 immunoblot but this finding was not confirmed in the reverse order.

BGJ398 resistant cell lines are selectively sensitive to tyrosine kinase inhibitors and to shRNA-mediated depletion of ERBB2 or ERBB3

To determine whether increased ERBB2 and ERBB3 signaling is necessary for acquired resistance to BGJ398, we examined whether ERBB inhibition suppressed growth of the resistant cells using a set of ERBB tyrosine kinase inhibitors. RT112 and BGJ398 resistant cells were exposed to AZD8931 (EGFR, ERBB2 and ERBB3 inhibitor), or lapatinib (EGFR and ERBB2 inhibitor) alone or in combination with 1 μ M BGJ398. The parental RT112 cells were sensitive to BGJ398 but showed little sensitivity to the ERBB family member inhibitors AZD8931 or lapatinib (Fig.3A presents data with AZD8931; Fig.S4 shows all inhibitor combinations). In contrast, the BGJ398 RS cell line was sensitive to AZD8931 and lapatinib and insensitive to BGJ398 (Fig.3A, and S4). Combined treatment with BGJ398 and AZD8931 resulted in increased growth inhibition in both the parental and resistant cell lines (Fig.3A), suggesting a potential ongoing co-dependency in both cases with a higher degree of FGFR dependency in the parental line and higher ERBB dependency in the resistant line. Similar results were observed for combinations of BGJ398 and lapatinib (Fig.S4).

Given that the inhibitor studies suggested a greater degree of FGFR dependence in RT112 and a greater degree of ERBB family member dependence in BGJ398 RS, we next sought to examine effects on signaling of ERBB and ERBB plus FGFR inhibition in the parental and resistant cell lines. The parental and resistant cells were treated with 1 μ M AZD8931 alone, 1 μ M BGJ398 alone, or the two drugs in combination and immunoblots were performed to assess the phosphorylation status of a number of signaling effectors. There was no acute toxicity associated with drug treatments at the assayed timepoint. We observed, as before, that p-FRS2 levels were high in the parental cell line (Fig.3B). p-FRS2 decreased with BGJ398 treatment but not AZD8931 (Fig.3B). There was little detectable p-FRS2 in BGJ398 RS as seen in Fig.S3. Basal levels of p-ERBB2 and p-ERBB3 were higher in BGJ398 RS as compared to RT112 and sensitive to AZD8931 treatment (Fig.3B). While AZD8931 alone inhibited p-AKT and p-ERK in BGJ398 RS it did not do so in the parental RT112 cells and a combination of BGJ398 and AZD8931 was required to observe a decrease in these signaling effectors, consistent with the concept co-dependency or rapid dependency switching in the parental line and a switch to a greater degree of ERBB dependency in BGJ398 RS (Fig.3B).

To address the roles of individual ERBB family members in acquired resistance to BGJ398, we expressed shRNAs targeting ERBB2 and ERBB3 using lentiviral vectors in the parental RT112 and BGJ398 RS. We screened a set of shRNA-expressing plasmids for the ability to knock down ERBB2 or ERBB3 protein (Figs. S5 and 3C). We then utilized the shRNA plasmids that drove the greatest depletion of the target and observed that knockdown of endogenous ERBB2 by these shRNAs led to a reduction in proliferation in both cell lines, but with a more robust reduction in BGJ398 RS cells than in parental cells (Fig.3C),

consistent with the inhibitor studies. The effects of ERBB3 depletion were more modest (Fig.S6A). ERBB3 was less effectively targeted by the shRNA, perhaps accounting in part for the more modest phenotypes as compared to ERBB2 knockdown (Fig.S6).

We next probed shRNA and drug combinations. In the parental cell lines we observed that knock-down of ERBB2 resulted in a modest decrease in viability which was potentiated by treatment with BGJ398 (Fig.3D, left panel). In contrast knock-down of ERBB2 had a greater effect on the viability of BGJ398 RS but there was no additional effect of adding BGJ398 (Fig.3D, left panel). AZD8931 led to death of BGJ398 RS but not parental RT112 cells expressing a shRNA targeting LacZ (Fig.3D, center panel). shERBB2 reduced proliferation of BGJ398 RS and the addition of AZD8931 increased this effect, consistent with a requirement for multiple ERBB family members in conferring resistance to BGJ398 (Fig. 3D, center panel). The combination of BGJ398 and AZD8931 led to substantial decreased viability in RT112 and BGJ398 RS in the presence or absence of shERBB2 (Fig.3D, right panel). A similar trend was seen in the same experiments performed in the context of ERBB3 depletion (Fig.S6B).

shRNA-mediated depletion of ERBB2 or ERBB3 leads to decreased migration and invasion in BGJ398 resistant cell lines

To assess whether ERBB2 and/or ERBB3 may be playing a role in the EMT-like phenotypes observed in Fig.1 we assessed cellular morphology, migration and invasion in BGJ398 RS cells in the context of shRNA-mediated depletion of either ERBB2 or ERBB3. ERBB2 depletion in BGJ398 RS cells led to a decrease in the spindle-like morphologic changes observed in BGJ398 RS cells expressing a shRNA targeting LacZ (Fig.4A, 40X magnification). Depletion of ERBB2 also blunted migration of BGJ398 RS cells in a scratch assay (Fig.4B) and invasion in matrigel (Fig.4C), consistent with partial loss of the EMT-like phenotype. Similar data were observed with ERBB3 depletion, though with more modest results. These data are presented in Fig.S7.

Acquired resistance to BGJ398 is reversible and correlated with increased production of ERBB ligands in independent cell line models

Other groups have shown that diverse mechanisms of acquired resistance to a single kinase inhibitor *in vitro* can be observed and may depend on how resistance is generated and may differ among kinase inhibitors with similar target selectivity profiles³⁴. To address this issue we established BGJ398 resistant RT112 cell lines both by stepwise escalation, as described above, and rapid exposure to high concentrations of BGJ398. We also used a second FGFR kinase inhibitor, ponatinib, to generate cell lines using the same protocol to address the generalizability of our results. The resulting BGJ398 RS (Resistant Stepwise) and BGJ398 RD (Resistant Direct) resistant cell lines as well as ponatinib RD and ponatinib RS were verified to be resistant to FGFR inhibition by both inhibitors using the Cell-Titer-Glo method (Fig.5A).

Interestingly, we again noted the EMT-like changes in the BGJ398 and ponatinib resistant RT112 cells derived by rapid inhibitor exposure, similar to what we observed in cells derived by stepwise exposure (Fig.1B). Given this observation and our previous experiments

which showed that ERBB activation occurs within one day of FGFR inhibition in RT112 cells, we reasoned that the acquired resistance may be due to changes in gene transcription and not due to the acquisition of additional somatic mutations, a process that can often take several weeks to arise. Consistent with this hypothesis, sensitivity to BGJ398 or ponatinib could be restored in the resistant cell lines by growth in the absence of drug for two to four weeks (resulting lines termed BGJ398 withdraw and ponatinib withdraw, Fig.5A) which was accompanied by a morphologic conversion back to the appearance of parental RT112 cells.

Since the time-frame for acquisition of resistance to FGFR inhibitors and the reversibility of this phenotype seemed more consistent with transcriptional changes as opposed to acquisition of novel mutations, we performed mRNA sequencing (RNAseq) on parental RT112 as well as the BGJ398 RS or BGJ398 RD cell lines and ponatinib RS and RD. As expected, we noted variable up-regulation of EGFR, ERBB2 and ERBB3 in all four of the resistant lines relative to the parental line, suggestive of a common mechanism of resistance (RNAseq data are presented in Supplementary Table1; validation by quantitative PCR in Fig.5B). We also observed that expression of NRG1, NRG2, NRG4, and BTC, ligands binding to ERBB family receptors, were also generally increased in the resistant cell lines (Fig.5B). Not all ERBB ligands were upregulated; for example, expression of EGF, HBEGF, AREG, and TGFA were unchanged or downregulated in the resistant lines (Figs 5B and Supplementary Table1). To further validate these findings we performed triplicate ELISA assays on the media from parental RT112 cells and BGJ398 RS. In agreement with the gene expression data, NRG1 protein was undetectable in the parental cell line and averaged 92.7 ± 9.4 pg/ml in BGJ398 RS and EGF was measured at 13.9 ± 0.03 pg/ml in RT112 and 4.5 ± 1.1 pg/ml in BGJ398 RS. NRG2 was undetectable in media from the parental RT112 line and just at the limits of detection in BGJ398 RS averaging 9.8 pg/ml, though the performance of the NRG2 ELISA assay was sub-optimal, suggesting that this result should be interpreted cautiously.

Ligand-mediated rescue

It has been previously demonstrated that bypass of dependence on RTKs can be achieved by ligand-mediated activation of alternative RTKs²⁵. Given that we observed that BGJ398 drives increased ERBB family activation and that BGJ398 and ponatinib impact the expression of ERBB ligands, we reasoned that ERBB ligands may be important in facilitating the dependency switch. We examined two *FGFR3* dependent cell lines, RT112 and RT4, and found that both lines were rendered resistant to BGJ398 treatment if grown in conditioned media from RT112 cells previously treated with BGJ398 (Fig.6A). In contrast two other cells lines with a high degree of sensitivity to FGFR inhibitors, the FGFR1 amplified cell line H1581 and FGFR2 amplified cell line Kato III, could not be rescued by the conditioned media (Fig.6A). Interestingly, we also obtained similar results using recombinant EGF in which the two *FGFR3* dependent lines could be rendered insensitive to BGJ398 treatment but not the *FGFR1* or *FGFR2* dependent line (Fig.S8). The effects of conditioned media on sensitivity to BGJ398 in RT112 cells could be blocked in part by a neutralizing antibody targeting NRG1 (Fig.S9A).

NRG1 can rescue cell from BGJ398 induced cell death in FGFR3-dependent cells

Our RNAseq data suggested that EGF was unlikely to be an important ERBB ligand in the setting of acquired resistance to FGFR inhibitors in the context of *FGFR3* dependency given that it was downregulated with BGJ398 treatment (Fig.5B, S Table1). NRG1, in contrast, is thought to be one of the principal ligands for stimulation of ERBB2/3 heterodimers³⁵ and was upregulated in our resistant cell lines (Fig.5B). Since ERBB2 and ERBB3 appeared to be upregulated both at the mRNA and protein level in resistant lines and also demonstrated greater degrees of phosphorylation, we sought to establish whether NRG1 alone could rescue BGJ398-induced death in RT112 and other FGFR dependent cell lines. Similar to our results from the conditioned media experiments and with EGF stimulation we observed that NRG1 rescued BGJ398-induced death in the *FGFR3* dependent lines RT112 and RT4 but not the FGFR1 dependent line H1581 or the *FGFR2* dependent line Kato III (Fig.6B). Additionally, we probed upregulated ERBB ligand NRG2 and noted that this ligand also demonstrated an observable but more modest degree of protection from BGJ398-induced cell death as compared to NRG1 in the *FGFR3* dependent cell lines (Fig.S9B). Addition of exogenous NRG1 or NRG2 was sufficient to drive upregulation of p-ERBB2 and p-ERBB3 in RT112 cells (Fig.S9C).

Discussion

The prevalence of somatic alterations of FGFRs in diverse types of cancer makes FGFRs attractive therapeutic targets. Given that the development of acquired resistance to targeted therapeutic drugs is a major obstacle in cancer medicine, we investigated mechanisms of acquired resistance to both selective and multi-targeted FGFR inhibitors. Using unbiased screening to examine the activity of RTKs in the setting of acquired resistance, we found that *ERBB2* and *ERBB3* were rapidly induced in cells treated with FGFR inhibitors and that resistant cells underwent a dependency switch from predominantly the FGFR to the ERBB signaling pathway, suggesting that signaling through ERBB2/3 can compensate for FGFR inhibition. This switching, in combination with the changes in cellular morphology and the production of ERBB receptor ligands was reversible, indicating substantial plasticity in the interaction among these oncogenic signaling pathways and suggesting a need for dual ERBB/FGFR inhibitors in this setting.

Acquired resistance to TKIs can arise through multiple mechanisms, typically involving second-site mutations in the target gene or by the activation of signaling pathways which bypass the original target^{30, 31, 36}. One commonly implicated bypass signaling pathway is driven by MET, implicated in resistance to FGFR and EGFR inhibitors^{25, 30, 31}. MET has been shown to drive EMT transitions and EMT has been observed in the setting of acquired resistance to EGFR directed therapy^{2, 37, 38, 39}. Recent data indicate that tumor EMT phenotypes are closely intertwined with the genomic alterations found in tumors and the response of cancers to targeted therapies. There are distinct “mesenchymal” and “epithelial” subsets of human bladder cancer cells. The “mesenchymal” phenotype is associated with *FGFR1* expression, while “epithelial” phenotype is associated with *FGFR3* expression and sensitivity to BGJ398 (ref.40). We also found *FGFR1* mRNA is up-regulated in BGJ398 resistant cells, along with the other mesenchymal markers which may account for the

resistance to FGFR inhibitors. Additionally, ERBB2 homo-dimerization and NRG1 secretion have been shown to cause EMT in mammary epithelial cells^{41, 42, 43}. Whether EMT is a cause or a result of acquired resistance is unclear and requires further study.

Our findings provide additional mechanistic insight into the ways in which tumors may develop resistance to FGFR inhibitors. Our study provides new details of how cancers may adapt to FGFR inhibition by activating ERBB2/3 in a rapid, reversible and ligand-dependent fashion. These results are similar to others obtained in the study of BRAF inhibitors in BRAF mutant melanoma and thyroid cancers^{44, 45}. Interestingly, these data appear only to apply to cancer cell lines dependent on *FGFR3* and not to other *FGFR* dependent models. This may be due to high basal expression of ERBB family members in these models which could allow more readily for dependency switching as compared to cell lines in which the ERBB signaling pathway is dormant. This may be similar to the case of HGF-driven resistance in which cell lines which displayed resistance to BGJ398 in the context of HGF were noted to express high basal levels of MET. It is likely that additional mechanisms of resistance to FGFR inhibitors will be described in *FGFR1* and *FGFR2* dependent cancers.

Our findings provide pre-clinical insights into acquired resistance to FGFR inhibitor-based therapy and suggest that dual FGFR/ERBB family inhibition is likely to be more effective than inhibiting either pathway alone in cancers which display either dependency switching or co-dependency. Given that several small molecule inhibitors and antibodies targeting ERBB family members are being studied in the clinic, it would be reasonable on the basis of our study and the work of others²⁶ to consider whether dual FGFR and ERBB therapy may be efficacious in FGFR-driven cancers. As several trials of FGFR inhibitors are underway we will soon learn if FGFR-ERBB dependency switching is observed in patient samples. We hope that these data will motivate additional studies of the response to FGFR inhibitors and mechanisms of resistance and also, together with the work of others, anticipate clinically relevant mechanisms of resistance.

Material and Methods

Cell culture and reagents

RT112, RT4, NCI-H1581 and Kato III were obtained from the core collection at Dana-Farber Cancer Institute or Broad Institute and were previously purchased from the American Type Culture Collection (ATCC). RT112, RT4 and Kato III cells were cultured in RPMI 1640, McCoy's 5a and DMEM plus 10% FBS. H1581 cells were cultured with ACL-4 medium (Invitrogen). BGJ398, ponatinib, AZD8931 and lapatinib were purchased from Selleck Chemicals. All compounds used in the in vitro experiments were prepared as 10mM stock solutions in dimethyl sulfoxide (DMSO).

Generation of drug resistant cell lines

Resistant cell lines were established by two different methods: RT112 parental cells were cultured with stepwise escalation of concentrations of BGJ398 or ponatinib from 4 nM to 1 μ M (stepwise escalation), with resulting resistant cells named BGJ398 RS or ponatinib RS,

or initially using a high concentration of BGJ398 or ponatinib (1 μ M) (high-concentration), with resulting resistant cells named BGJ398 RD or ponatinib RD.

Cell proliferation and Viability assays

Cell proliferation was measured with the Cell-Titer-Glo reagent (Promega) following the manufacturer's instructions. Cells were plated into flat-bottomed 96-well plates at a density of 1,500 cells per well and were treated the next day with compound or vehicle (DMSO) for 96 hours. Proliferation measurements were made using a luminometer. Data are shown as relative values in which the luminescence at a given drug concentration is compared with that of untreated cells.

Cell migration and Transwell invasion assays

For the scratch migration assay, cells were grown to confluence in a monolayer in 6-well plates. A linear gap was generated and BGJ398 were added at a final concentration of 1 μ M or vehicle into the medium. Microscopic images were acquired at 0 and 24 hours. For the transwell migration assay, BD BioCoat invasion chambers (8- μ m pore size) coated with Matrigel were used. Cells were serum starved overnight and resuspended in RPMI 1640 containing 0.1% FBS. These cells (2.5×10^5 cells/chamber) were then added to the top chambers, whereas the bottom chambers contained RPMI 1640 with 10% FBS. BGJ398 was added on the top chambers at a final concentration of 1 μ M. After 24 hours of incubation, the membranes were fixed with methanol and stained with DAPI. The number of migrated cells was quantified by counting five random distinct fields under a microscope at 40x magnification. The number of migrated control cells was taken as 100%.

Phospho-receptor tyrosine kinase (RTK) array

The activity of a panel of RTKs was screened using an antibody-based array from R&D Systems (Minneapolis, MN) according to the manufacturer's instructions. The parental cells or BGJ398 RS cells were treated with 1 μ M BGJ398 for 1 hour and the cell lysates were incubated with the membrane. Thereafter, a pan anti-phospho-tyrosine antibody was used to detect the phosphorylated tyrosine on activated RTKs.

Immunoblotting analysis

Following treatment, cells were lysed in RIPA. Equal amounts of protein were analyzed by SDS-PAGE. Primary antibodies used were as follows: Phospho-FGF Receptor (Tyr653/654, 55H2, #3476S), FGF Receptor 3 (C51F2, #4574S), Phospho-FRS2- α (Tyr436, #3861S), Phospho-ERBB2 (Y1221/1222, #2243S), Phospho-ERBB3 (Y1289, #4791S), Phospho-EGFR (Y1068, 1H12, #2236S), AKT (#9272S), Phospho-AKT (Ser473, D9E, #4060S), Phospho-ERK1/2(T202/Y204, #4370S), ERK1/2 (137F5, #4695S) were from Cell Signaling Technologies. FRS2 (H-91, sc-8318) was purchased from Santa Cruz. ERBB2 (e2-4001) was from NeoMarkers, ERBB3 (#MA5-12675) was from Thermo Scientific. EGFR (#A300-388A) was from Bethyl Antibodies.

ShRNA constructs and lentiviral infection

ERBB2 and ERBB3 shRNA were obtained from TRC (RNAi Consortium at the Broad Institute, Cambridge, MA)⁴⁶. The target sequence of the shRNA constructs are: ERBB2: TGTCAGTATCCAGGCTTTGTA, ERBB3: GCCTACCAGTTGGAACACTTA. A vector containing LacZ sequence was used as controls. Lentiviral infections were performed according to the online TRC protocol (<http://www.broadinstitute.org/rnai/public/resources/protocols>) with 293T cells transfected with the suggested 3-vector combination. Virus was collected and used to infect the RT112 or BGJ398 RS cell lines for 6 hours in the presence of 8 µg/ml polybrene. Stable cell lines were generated using puromycin selection at a concentration of 2 µg/ml. Knockdown were confirmed by immunoblot.

Immunoprecipitation

For the detection of ERBB2/ERBB3 dimerization, whole-cell lysates (1mg) in NP40 lysis buffer was incubated with agarose A/G plus pre-conjugated with the ERBB2 or ERBB3 antibody. Immunoprecipitates were washed in lysis buffer, boiled in sample buffer, and subjected to SDS-PAGE followed by immunoblotting using an anti-ERBB2 or anti-ERBB3 or anti-EGFR to detect specific dimerization of ERBB family members.

RNA sequencing (RNAseq) analysis

Total RNA was prepared using the Qiagen RNeasy kit. Libraries were prepared using the NEBNext library Prep Kit (New England Biolabs) according to the manufacturer's instructions. Library quality was assessed using a Bioanalyzer (Agilent) and then were sequenced on the Illumina HiSeq 2000 with a goal of 30 million reads per sample. Raw FASTQ files were aligned using PRADA and FPKM values obtained using Cufflinks for gene expression analysis.

Real-time PCR

Total RNA was reverse-transcribed into cDNA using the iScript cDNA Synthesis Kit (Bio-rad). Quantitative real-time PCR (q-PCR) analysis was performed using a MyiQ real time PCR Detection System (Bio-rad) and the SYBR Green q-PCR kit (Bio-Rad, Hercules, CA). GAPDH mRNA levels were used as internal controls in the qRT-PCR analysis.

Enzyme-linked immunosorbent assay (ELISA)

The supernatant was collected from parental and BGJ398 RS cell line 48 hours after media change, and stored at -80°C until measurement. The ERBB family ligands NRG1, NRG2, NRG4 and EGF were measured using the ELISA kit (Abnova for NRG1, Cloud-clone for NRG2 and NRG4, R&D for EGF) according to the manufacturer's instructions.

Statistical analysis

All data are expressed with mean ± standard deviation (SD), IC50 values were obtained using GraphPad Prism software. Statistical significance was calculated by Student's t test, considering $P < 0.05$ as statistically significant.

Supplementary Material

Refer to Web version on PubMed Central for supplementary material.

Acknowledgements

P.S. Hammerman is supported by NCI K08 CA163677, the V Foundation the Stephen D. and Alice Cutler Fund. We thank M. Meyerson for assisting with the planning of this study. J. Wang is supported by NSFC 81202746 and CSC.

Financial Support: P.S. Hammerman is supported by NCI K08 CA163677, the V Foundation and the Stephen D. and Alice Cutler Fund. J. Wang is supported by NSFC 81202746 and CSC.

References

- Dieci MV, Arnedos M, Andre F, Soria JC. Fibroblast growth factor receptor inhibitors as a cancer treatment: from a biologic rationale to medical perspectives. *Cancer discovery*. 2013; 3:264–279. [PubMed: 23418312]
- Katoh M, Nakagama H. FGF Receptors: Cancer Biology and Therapeutics. *Medicinal research reviews*. 2013
- Turner N, Grose R. Fibroblast growth factor signalling: from development to cancer. *Nature reviews Cancer*. 2010; 10:116–129. [PubMed: 20094046]
- Weiss J, Sos ML, Seidel D, Peifer M, Zander T, Heuckmann JM, et al. Frequent and focal FGFR1 amplification associates with therapeutically tractable FGFR1 dependency in squamous cell lung cancer. *Science translational medicine*. 2010; 2:62ra93.
- Hammerman PS, Hayes DN, Wilkerson MD, Schultz N, Bose R, Chu A, et al. Comprehensive genomic characterization of squamous cell lung cancers. *Nature*. 2012; 489:519–525. [PubMed: 22960745]
- Courjal F, Cuny M, Simony-Lafontaine J, Louason G, Speiser P, Zeillinger R, et al. Mapping of DNA amplifications at 15 chromosomal localizations in 1875 breast tumors: definition of phenotypic groups. *Cancer research*. 1997; 57:4360–4367. [PubMed: 9331099]
- Kunii K, Davis L, Gorenstein J, Hatch H, Yashiro M, Di Bacco A, et al. FGFR2-amplified gastric cancer cell lines require FGFR2 and Erbb3 signaling for growth and survival. *Cancer research*. 2008; 68:2340–2348. [PubMed: 18381441]
- Turner N, Lambros MB, Horlings HM, Pearson A, Sharpe R, Natrajan R, et al. Integrative molecular profiling of triple negative breast cancers identifies amplicon drivers and potential therapeutic targets. *Oncogene*. 2010; 29:2013–2023. [PubMed: 20101236]
- van Rhijn BW, van Tilborg AA, Lurkin I, Bonaventure J, de Vries A, Thiery JP, et al. Novel fibroblast growth factor receptor 3 (FGFR3) mutations in bladder cancer previously identified in non-lethal skeletal disorders. *European journal of human genetics : EJHG*. 2002; 10:819–824. [PubMed: 12461689]
- Dutt A, Salvesen HB, Chen TH, Ramos AH, Onofrio RC, Hatton C, et al. Drug-sensitive FGFR2 mutations in endometrial carcinoma. *Proceedings of the National Academy of Sciences of the United States of America*. 2008; 105:8713–8717. [PubMed: 18552176]
- Liao RG, Jung J, Tchaicha J, Wilkerson MD, Sivachenko A, Beauchamp EM, et al. Inhibitor-Sensitive FGFR2 and FGFR3 Mutations in Lung Squamous Cell Carcinoma. *Cancer research*. 2013; 73:5195–5205. [PubMed: 23786770]
- Chesi M, Nardini E, Brents LA, Schrock E, Ried T, Kuehl WM, et al. Frequent translocation t(4;14)(p16.3;q32.3) in multiple myeloma is associated with increased expression and activating mutations of fibroblast growth factor receptor 3. *Nature genetics*. 1997; 16:260–264. [PubMed: 9207791]
- Chesi M, Brents LA, Ely SA, Bais C, Robbiani DF, Mesri EA, et al. Activated fibroblast growth factor receptor 3 is an oncogene that contributes to tumor progression in multiple myeloma. *Blood*. 2001; 97:729–736. [PubMed: 11157491]

14. Singh D, Chan JM, Zoppoli P, Niola F, Sullivan R, Castano A, et al. Transforming fusions of FGFR and TACC genes in human glioblastoma. *Science*. 2012; 337:1231–1235. [PubMed: 22837387]
15. Williams SV, Hurst CD, Knowles MA. Oncogenic FGFR3 gene fusions in bladder cancer. *Human molecular genetics*. 2013; 22:795–803. [PubMed: 23175443]
16. Majewski IJ, Mittempergher L, Davidson NM, Bosma A, Willems SM, Horlings HM, et al. Identification of recurrent FGFR3 fusion genes in lung cancer through kinome-centred RNA sequencing. *The Journal of pathology*. 2013; 230:270–276. [PubMed: 23661334]
17. Wu YM, Su F, Kalyana-Sundaram S, Khazanov N, Ateeq B, Cao X, et al. Identification of targetable FGFR gene fusions in diverse cancers. *Cancer discovery*. 2013; 3:636–647. [PubMed: 23558953]
18. Lamont FR, Tomlinson DC, Cooper PA, Shnyder SD, Chester JD, Knowles MA. Small molecule FGF receptor inhibitors block FGFR-dependent urothelial carcinoma growth in vitro and in vivo. *British journal of cancer*. 2011; 104:75–82. [PubMed: 21119661]
19. Lemieux S, Hadden MK. Targeting the fibroblast growth factor receptors for the treatment of cancer. *Anti-cancer agents in medicinal chemistry*. 2013; 13:748–761. [PubMed: 23272905]
20. Andre F, Bachelot T, Campone M, Dalenc F, Perez-Garcia JM, Hurvitz SA, et al. Targeting FGFR with dovitinib (TKI258): preclinical and clinical data in breast cancer. *Clinical cancer research : an official journal of the American Association for Cancer Research*. 2013; 19:3693–3702. [PubMed: 23658459]
21. Wolf J, LoRusso PM, Camidge RD, Perez JM, Tabernero J, Hidalgo M, et al. Abstract LB-122: A phase I dose escalation study of NVP-BGJ398, a selective pan FGFR inhibitor in genetically preselected advanced solid tumors. *Cancer research*. 2012; 72
22. Guagnano V, Furet P, Spanka C, Bordas V, Le Douget M, Stamm C, et al. Discovery of 3-(2,6-dichloro-3,5-dimethoxy-phenyl)-1-{6-[4-(4-ethyl-piperazin-1-yl)-phenyl]amino}-pyrimidin-4-yl}-1-methyl-urea (NVP-BGJ398), a potent and selective inhibitor of the fibroblast growth factor receptor family of receptor tyrosine kinase. *Journal of medicinal chemistry*. 2011; 54:7066–7083. [PubMed: 21936542]
23. Guagnano V, Kauffmann A, Wohrle S, Stamm C, Ito M, Barys L, et al. FGFR genetic alterations predict for sensitivity to NVP-BGJ398, a selective pan-FGFR inhibitor. *Cancer discovery*. 2012; 2:1118–1133. [PubMed: 23002168]
24. Garraway LA, Janne PA. Circumventing cancer drug resistance in the era of personalized medicine. *Cancer discovery*. 2012; 2:214–226. [PubMed: 22585993]
25. Harbinski F, Craig VJ, Sanghavi S, Jeffery D, Liu L, Sheppard KA, et al. Rescue screens with secreted proteins reveal compensatory potential of receptor tyrosine kinases in driving cancer growth. *Cancer discovery*. 2012; 2:948–959. [PubMed: 22874768]
26. Herrera-Abreu MT, Pearson A, Campbell J, Shnyder SD, Knowles MA, Ashworth A, et al. Parallel RNA Interference Screens Identify EGFR Activation as an Escape Mechanism in FGFR3-Mutant Cancer. *Cancer discovery*. 2013; 3:1058–1071. [PubMed: 23744832]
27. Chell V, Balmanno K, Little AS, Wilson M, Andrews S, Blockley L, et al. Tumour cell responses to new fibroblast growth factor receptor tyrosine kinase inhibitors and identification of a gatekeeper mutation in FGFR3 as a mechanism of acquired resistance. *Oncogene*. 2013; 32:3059–3070. [PubMed: 22869148]
28. Sequist LV, Waltman BA, Dias-Santagata D, Digumarthy S, Turke AB, Fidias P, et al. Genotypic and histological evolution of lung cancers acquiring resistance to EGFR inhibitors. *Science translational medicine*. 2011; 3:75ra26.
29. Hanahan D, Weinberg RA. Hallmarks of cancer: the next generation. *Cell*. 2011; 144:646–674. [PubMed: 21376230]
30. Engelman JA, Zejnullahu K, Mitsudomi T, Song Y, Hyland C, Park JO, et al. MET amplification leads to gefitinib resistance in lung cancer by activating ERBB3 signaling. *Science*. 2007; 316:1039–1043. [PubMed: 17463250]
31. Wilson TR, Fridlyand J, Yan Y, Penuel E, Burton L, Chan E, et al. Widespread potential for growth-factor-driven resistance to anticancer kinase inhibitors. *Nature*. 2012; 487:505–509. [PubMed: 22763448]

32. Schlessinger J. Ligand-induced, receptor-mediated dimerization and activation of EGF receptor. *Cell*. 2002; 110:669–672. [PubMed: 12297041]
33. Bublil EM, Yarden Y. The EGF receptor family: spearheading a merger of signaling and therapeutics. *Current opinion in cell biology*. 2007; 19:124–134. [PubMed: 17314037]
34. Shien K, Toyooka S, Yamamoto H, Soh J, Jida M, Thu KL, et al. Acquired resistance to EGFR inhibitors is associated with a manifestation of stem cell-like properties in cancer cells. *Cancer research*. 2013; 73:3051–3061. [PubMed: 23542356]
35. Citri A, Skaria KB, Yarden Y. The deaf and the dumb: the biology of ErbB-2 and ErbB-3. *Experimental cell research*. 2003; 284:54–65. [PubMed: 12648465]
36. Straussman R, Morikawa T, Shee K, Barzily-Rokni M, Qian ZR, Du J, et al. Tumour micro-environment elicits innate resistance to RAF inhibitors through HGF secretion. *Nature*. 2012; 487:500–504. [PubMed: 22763439]
37. Barr S, Thomson S, Buck E, Russo S, Petti F, Sujka-Kwok I, et al. Bypassing cellular EGF receptor dependence through epithelial-to-mesenchymal-like transitions. *Clinical & experimental metastasis*. 2008; 25:685–693. [PubMed: 18236164]
38. Winter SF, Acevedo VD, Gangula RD, Freeman KW, Spencer DM, Greenberg NM. Conditional activation of FGFR1 in the prostate epithelium induces angiogenesis with concomitant differential regulation of Ang-1 and Ang-2. *Oncogene*. 2007; 26:4897–4907. [PubMed: 17297442]
39. Zhang Z, Lee JC, Lin L, Olivás V, Au V, LaFramboise T, et al. Activation of the AXL kinase causes resistance to EGFR-targeted therapy in lung cancer. *Nature genetics*. 2012; 44:852–860. [PubMed: 22751098]
40. Cheng T, Roth B, Choi W, Black PC, Dinney C, McConkey DJ. Fibroblast growth factor receptors-1 and -3 play distinct roles in the regulation of bladder cancer growth and metastasis: implications for therapeutic targeting. *PloS one*. 2013; 8:e57284. [PubMed: 23468956]
41. Jenndahl LE, Isakson P, Baeckstrom D. c-erbB2-induced epithelial-mesenchymal transition in mammary epithelial cells is suppressed by cell-cell contact and initiated prior to E-cadherin downregulation. *International journal of oncology*. 2005; 27:439–448. [PubMed: 16010426]
42. Lu J, Guo H, Treekitkarnmongkol W, Li P, Zhang J, Shi B, et al. 14-3-3zeta Cooperates with ErbB2 to promote ductal carcinoma in situ progression to invasive breast cancer by inducing epithelial-mesenchymal transition. *Cancer cell*. 2009; 16:195–207. [PubMed: 19732720]
43. Kim J, Jeong H, Lee Y, Kim C, Kim H, Kim A. HRG-beta1-driven ErbB3 signaling induces epithelial-mesenchymal transition in breast cancer cells. *BMC cancer*. 2013; 13:383. [PubMed: 23937725]
44. Abel EV, Basile KJ, Kugel CH 3rd, Witkiewicz AK, Le K, Amaravadi RK, et al. Melanoma adapts to RAF/MEK inhibitors through FOXD3-mediated upregulation of ERBB3. *The Journal of clinical investigation*. 2013; 123:2155–2168. [PubMed: 23543055]
45. Montero-Conde C, Ruiz-Llorente S, Dominguez JM, Knauf JA, Viale A, Sherman EJ, et al. Relief of feedback inhibition of HER3 transcription by RAF and MEK inhibitors attenuates their antitumor effects in BRAF-mutant thyroid carcinomas. *Cancer discovery*. 2013; 3:520–533. [PubMed: 23365119]
46. Moffat J, Grueneberg DA, Yang X, Kim SY, Kloepfer AM, Hinkle G, et al. A lentiviral RNAi library for human and mouse genes applied to an arrayed viral high-content screen. *Cell*. 2006; 124:1283–1298. [PubMed: 16564017]

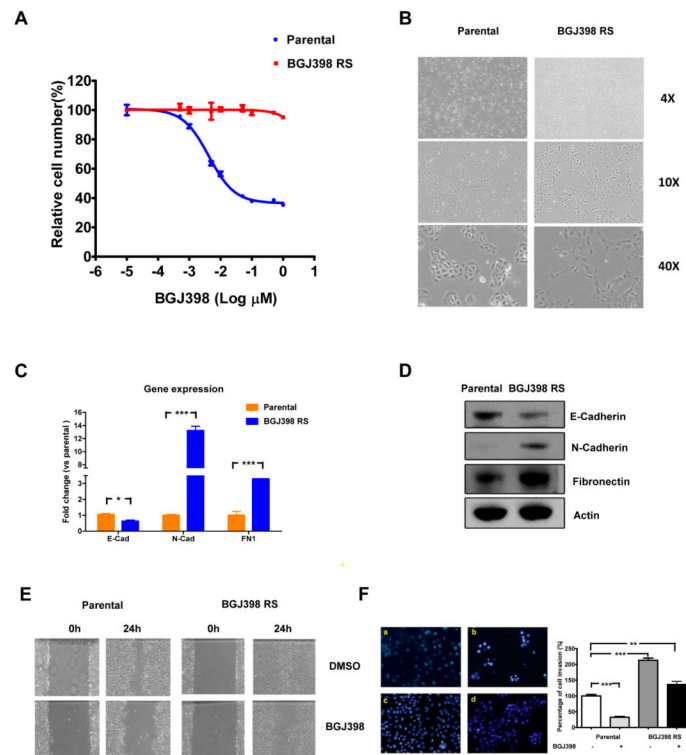


Fig. 1. RT112 RS cells are resistant to BGJ398 in vitro and demonstrate EMT-like properties (A) The *FGFR3* dependent RT112 human bladder cell line was made resistant to BGJ398 by growth in increasing concentrations of BGJ398. The resistance was confirmed by dose response curve. Cells were treated with the indicated concentration of BGJ398 for 4 days and growth was measured using the growth proliferation assay and plotted as a percentage of growth relative to untreated control cells. Data points are represented as Mean \pm SD (n=3). (B) Parental and BGJ398 resistant cells display different morphology under light microscope. (C) q-PCR analysis shows differential expression levels of EMT-related genes in parental and BGJ398 RS cells. (D) Immunoblots of candidate EMT related proteins. (E) Cell migration assay. A wound was produced on the cell layer with a pipette tip and the parental and BGJ398 resistant cells incubated with or without 1 μ M BGJ398. Wound repair after 24 hours of stimulation was observed under a microscope. (F) Cell invasion was examined using a Boyden chamber assay. Serum free parental cell and resistant cells were seeded on the top of the chamber, with or without exposure to 1 μ M BGJ398. Media containing 10% FBS was added into the lower chamber. After 24 hours, the invading cells were stained with DAPI and the number of cells manually counted. 3 independent experiments and five microscopic fields were counted per insert. The number of migrated control cells was taken as 100%. The experiments were repeated at least twice. *, $P < 0.05$; **, $P < 0.01$ ***, $P < 0.001$ compared with indicated group.

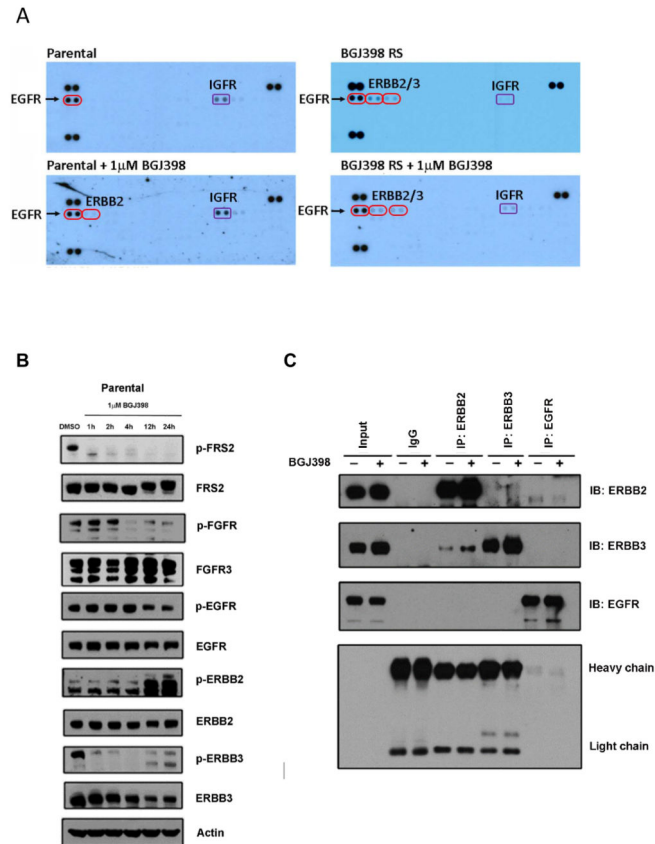


Fig. 2. Activation of ERBB2 and ERBB3 in BGJ398 RS cells

(A) A phospho-RTK array reveals that BGJ398 RS cells have increased phosphorylation of ERBB2 and ERBB3 in the presence of BGJ398. The cell lysates were hybridized to a phospho-RTK membrane, on which each RTK is spotted in duplicate. Hybridization signals at the corners serve as controls. (B) Immunoblot analysis of protein phosphorylation in extracts from parental cells that were treated for the indicated time points with 1µM BGJ398. (C) ERBB2 and ERBB3 dimerization measured by co-immunoprecipitation. The parental cells were treated with 1µM BGJ398 for 24h and prior to lysis. The experiments were performed at least twice.

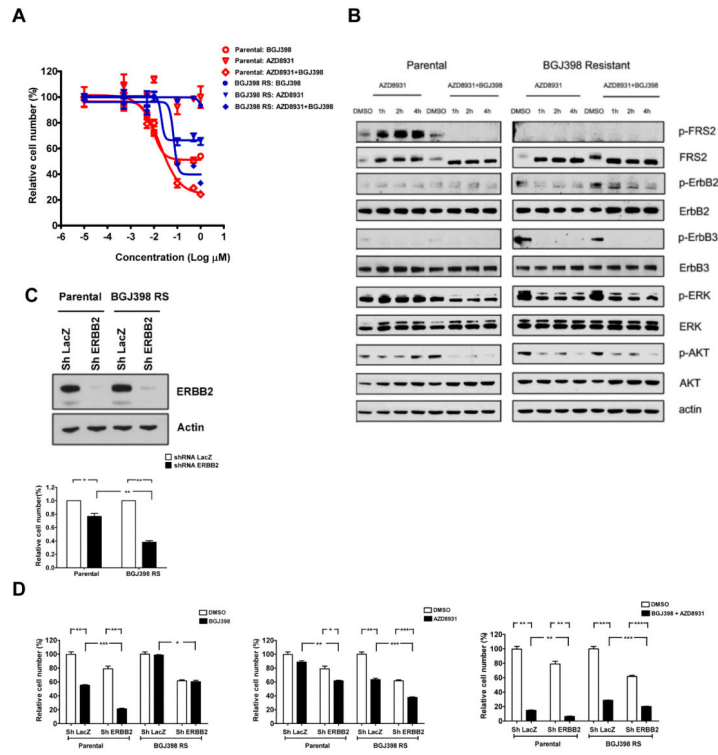


Fig. 3. BGJ398 RS cell lines are selectively sensitive to tyrosine kinase inhibitors and to shRNA-mediated depletion of ERBB2 or ERBB3

A) BGJ398 RS cells are sensitive to the ERBB family inhibitor. Parental and BGJ398 RS cells were exposed to BGJ398 or AZD8931 alone or in combination, and cell proliferation was measured 4 days after treatment using Cell-Titer-GLO. (B) Immunoblot analysis of protein phosphorylation in extracts from parental and BGJ398 RS cells that were treated for indicated time point with 1 μ M BGJ398, 1 μ M AZD8931 or a combination of both drugs. (C) Upper: Immunoblots demonstrate down-regulation of ERBB2 by the specific shRNA. A lacZ control or ERBB2 specific shRNAs were introduced into parental or BGJ398 RS cells. Cells underwent puromycin selection and extracts were immunoblotted with the indicated antibodies. Lower: BGJ398 RS cells are sensitive to knock-down of ERBB2 expression. The number of cells were counted 72 hours after seeding, and the viability of knockdown samples (in triplicate) is presented relative to LacZ control sample. (D) Knockdown of ERBB2 also sensitizes the BGJ398 RS cells to AZD8931. Parental and BGJ398 RS cells were infected with indicated shRNA and the proliferation is shown for indicated cells treated for 96 hours with 1 μ M BGJ398, 1 μ M AZD8931 or a combination of both drugs. Proliferation is shown relative to untreated cells at the same time point. The experiments were repeated twice. *, $P < 0.05$; **, $P < 0.01$; ***, $P < 0.001$ compared with indicated group.

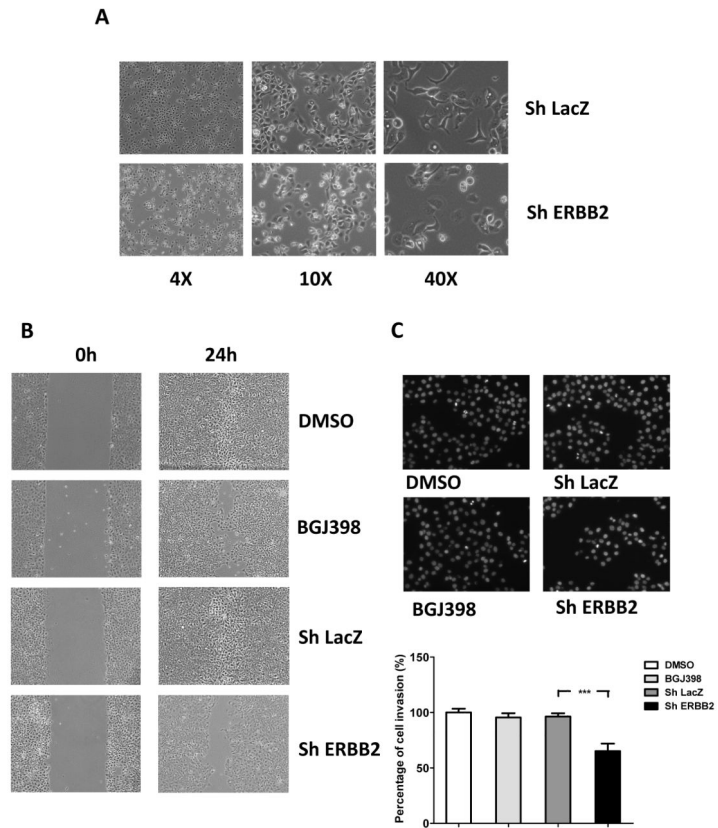


Fig. 4. shRNA-mediated depletion of ERBB2 leads to decreased migration and invasion in BGJ398 resistant cell lines

BGJ398 RS cells were infected with shRNA targeting ERBB2 as in Fig.3 or LacZ control. The morphology (A), as well as cell migration (B), and invasion (C) assay were monitored as previously described in Fig.1. The experiments were performed in triplicate. ***, $P < 0.001$.

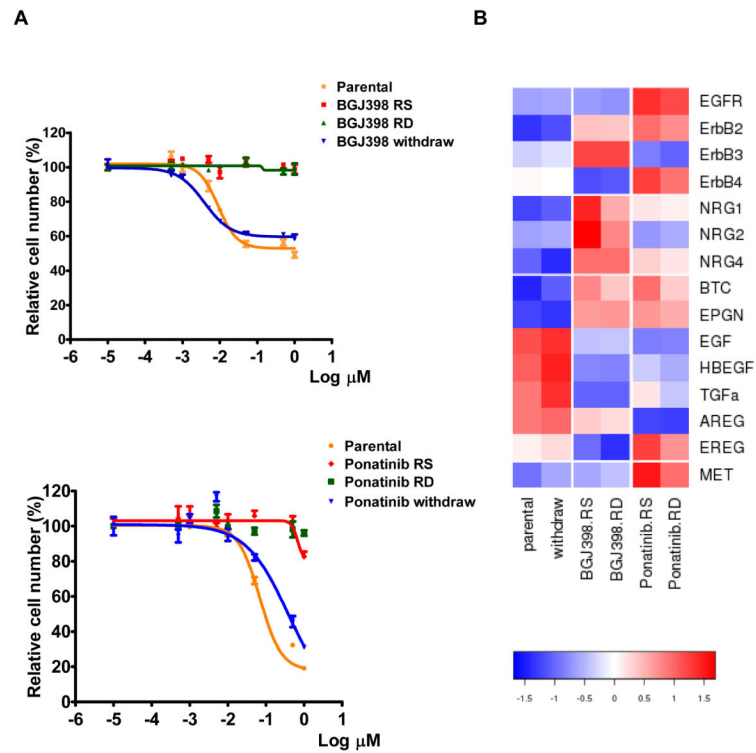


Fig. 5. Acquired resistance to BGJ398 is reversible and correlated with increased production of ERBB ligands

(A) Four resistant cell lines were generated by either stepwise escalation (RS) or high-concentration exposure (RD) to either BGJ398 or ponatinib. Both BGJ398 RS, BGJ398 RD, Ponatinib RS and Ponatinib RD cell lines were verified to be resistant by the Cell-Titer-Glo method. This resistance was reversible as the cells were sensitive to BGJ398 or ponatinib again after drug withdrawal for two to four weeks (BGJ withdraw and ponatinib withdraw).

(B) Heatmap representation of the expression of ERBB family members as well as their ligands as determined by q-PCR. The experiments were repeated twice.

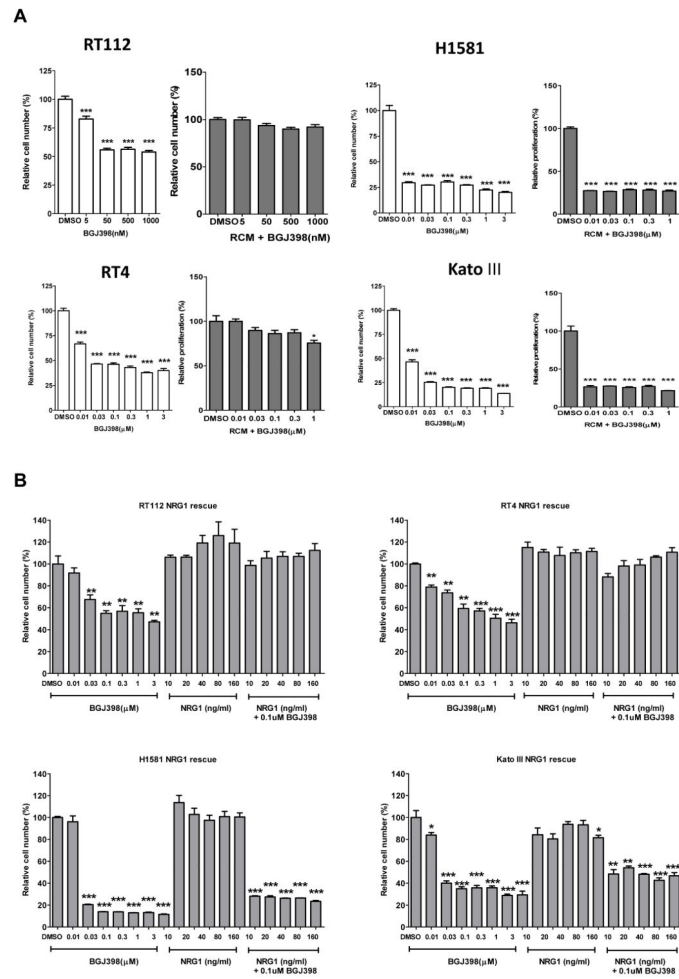


Fig. 6. Conditioned media and Ligand-mediated rescue

(A) RT112 and RT4 (FGFR3 dependent), H1581 (FGFR1 dependent), and Kato III (FGFR2 dependent) cells were rescued by conditioned medium collected from BGJ398 RS cell line (RCM). The conditioned medium was collected from BGJ398 RS cells, at 48 hours after media change, and then mixed with fresh media at a 1:1 ratio. Proliferation was measured 96 hours after drug treatment. (B) Cells were treated with the indicated concentrations of recombinant NRG1 in the presence or absence of BGJ398. All cells were treated for 96 hours, and relative cell growth was quantified using Cell-Titer-Glo readout. The experiments were performed in triplicate and repeated at least twice. *, $P < 0.05$; **, $P < 0.01$; ***, $P < 0.001$ compared with DMSO group.